

Inelastic Electron Tunneling Spectroscopy of Molecular Transport Junctions

Hyunwook SONG*

Department of Applied Physics, Kyung Hee University, Yongin 446-701, Korea

Takhee LEE†

Department of Physics and Astronomy, Seoul National University, Seoul 151-744, Korea

Mark REED‡

Departments of Electrical Engineering and Applied Physics Yale University, New Haven, CT 06520, USA

(Received 22 October 2013, in final form 19 January 2014)

Inelastic electron tunneling spectroscopy (IETS) has become a premier analytical tool in the investigation of nanoscale and molecular junctions. The IETS spectrum provides invaluable information about the structure, bonding, and orientation of component molecules in the junctions. One of the major advantages of IETS is its sensitivity and resolution at the level of single molecules. This review discusses how IETS is used to study molecular transport junctions and presents an overview of recent experimental studies.

PACS numbers: 73.63.Rt, 81.07.Nb

Keywords: Inelastic electron tunneling spectroscopy, Molecular electronics, Molecular junctions

DOI: 10.3938/jkps.64.1539

I. INTRODUCTION

Molecular transport junctions are a basic building block of molecular electronic devices, and that building block consists of one or very few molecules contacted between metallic electrodes [1–8], as shown in Fig. 1. Inelastic electron tunneling spectroscopy (IETS) is a unique spectroscopic technique which has shown great sensitivity and resolution (of a single molecule level) in studies of the vibration spectra of the constituent molecules in a molecular junction [9–14]. The physical process underlying IETS is the inelastic interaction of a tunneling electron with intrinsic molecular vibrations [9–11]. The technique can detect vibration modes of molecules through such inelastic tunneling processes, and the fully-assigned IETS spectra can be used to identify the chemical species existing in a current-carrying molecular junction and even to determine their conformation and orientation. IETS is becoming a powerful tool for studies of molecular electronics [11] and surface and interfacial phenomena [15]. This review gives a brief description of the principle of IETS (Section II) and discusses recent experimental research which utilizes IETS as an analytical tool for the investigation of molecular

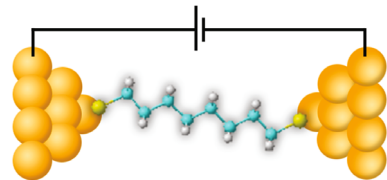


Fig. 1. (Color online) Illustration of a single molecule (1,8-octanedithiol) attached to metallic electrodes as a basic component in molecular electronic devices.

transport junctions (Section III).

II. BASIC PRINCIPLE OF INELASTIC ELECTRON TUNNELING SPECTROSCOPY

Inelastic electron tunneling spectroscopy (IETS), an all-electronic spectroscopy that employs localized molecular vibrational modes, was discovered in 1966 by Jaklevic and Lambe [10]. This pioneering work clearly showed the ability to detect the vibrational features of molecules buried in the interface of a metal-insulator-metal (MIM) device. To explain the principles of IETS, Fig. 2 shows the energy-band diagrams of a tunnel junction and the corresponding $I(V)$, dI/dV , and d^2I/dV^2 plots [11]. When a negative bias (small with respect to

*E-mail: hsong@khu.ac.kr; Fax: +82-31-204-8122

†E-mail: tlee@snu.ac.kr

‡E-mail: mark.reed@yale.edu

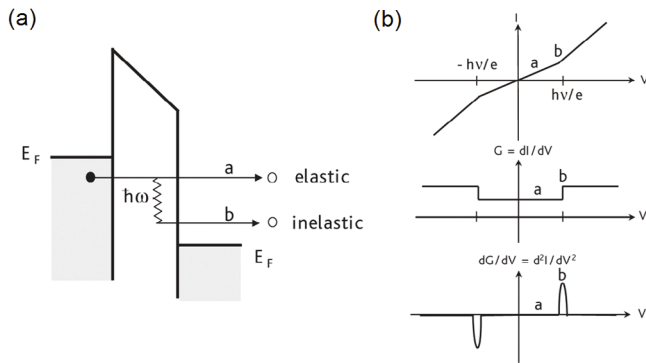


Fig. 2. (a) Energy band diagram of a tunnel junction with a vibrational mode of frequency ω localized inside: ‘a’ is the elastic tunneling process and ‘b’ is the inelastic tunneling process. (b) Corresponding $I(V)$, dI/dV , and d^2I/dV^2 characteristics. Reprinted with permission from [11], Copyright 2008 Elsevier.

the tunnel barrier) is applied to the left metal electrode, the left Fermi level is elevated. An electron from an occupied state on the left side then tunnels into an empty state on the right side, and its energy is conserved (process a). This process is called elastic tunneling. During this mechanism, the current increases linearly with an applied small bias (less than the vibrational energy) (Fig. 2(b)). However, if a vibrational mode with a frequency of ω is localized inside this barrier, then the electron can lose a quantum of energy, $\hbar\omega$, to excite the vibrational mode and can tunnel into another empty state when the applied bias is so large that $eV \geq \hbar\omega$ (process b). This process opens an inelastic tunneling channel for the electron, and its overall tunneling probability is increased. Thus, the total tunneling current has a kink that is a function of the applied bias (Fig. 2(b)). This kink becomes a step in the differential conductance (dI/dV) plot and a peak in the d^2I/dV^2 plot. Typically, only a very small fraction of electrons tunnel inelastically (the cross-section for such an excitation is very small because the electron traversal time is much smaller than the oscillator period), and thus the IETS conductance step is often too small to be conveniently detected. In practice, a phase-sensitive (“lock-in”) detection technique is used to directly measure the peaks of the second derivative of $I(V)$. Theoretically, the signal can also be determined by a mathematical differential approach that computes the numerical derivatives of the directly measured $I(V)$ characteristics [16]. However, this method is generally not feasible in practice due to the insufficient signal-to-noise ratios or bit resolutions of the instrumentation used to acquire the data. In addition, there is an orientation preference in IETS, but there are no rigorous selection rules for infrared or Raman spectroscopy. Both infrared- and Raman-active vibrational modes can appear in IETS spectra.

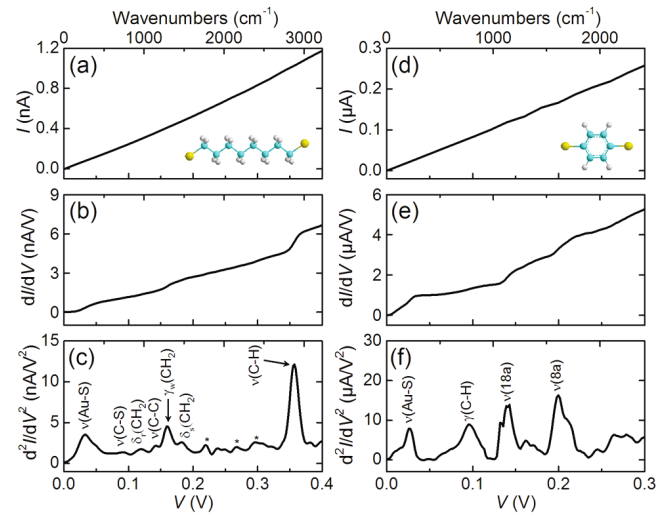


Fig. 3. (Color online) Transport properties of Au-ODT-Au [(a)–(c)] and Au-BDT-Au [(d)–(f)] junctions measured at 4.2 K. [(a) and (d)] $I(V)$ characteristics. The insets display the chemical structure of each molecule. [(b) and (e)] Differential conductance (dI/dV) obtained from the lock-in first harmonic signal. [(c) and (f)] IETS spectrum (d^2I/dV^2) obtained from the lock-in second harmonic signal. The peaks are labeled with their assigned vibrational modes. Reprinted with permission from [17], Copyright 2009 American Institute of Physics.

III. INELASTIC ELECTRON TUNNELING SPECTROSCOPY FOR INVESTIGATING MOLECULAR TRANSPORT JUNCTIONS

IETS has recently become a primary characterization technique to identify the component molecules present in molecular junctions (not an adlayer or impurity, but molecules forming the active region of a junction) [17–22], analogous to infrared and Raman spectroscopy for macroscopic samples, for an unambiguous determination of the molecular species in the junction. An example of experimental IETS measurements is shown in Fig. 3 [17], which shows the $I(V)$ curve, the differential conductance (dI/dV), and the IETS (d^2I/dV^2) spectrum of Au-1,8-octanedithiol (ODT)-Au and Au-1,4-benzenedithiol (BDT)-Au junctions measured at 4.2 K by using an electromigrated break junction. Although the $I(V)$ characteristics seem to be linear over the bias range measured, the plots of dI/dV and d^2I/dV^2 exhibit significant features corresponding to vibrational modes of the molecules under investigation. Standard AC modulation techniques with a lock-in amplifier are used to directly obtain the first- and the second-harmonic signals proportional to dI/dV and d^2I/dV^2 , respectively. As explained above, a molecular vibration coupled to tunneling charge carriers gives rise to an increase in the slope of the dI/dV curve owing to an inelastic tunneling process, which then appears as a step and a peak in the first (dI/dV) and the second (d^2I/dV^2) derivatives, respectively. The plot of

d^2I/dV^2 versus V is referred to as the IETS spectrum. The observed spectral features were assigned to specific molecular vibrations by comparisons with previously reported infrared, Raman, and IETS measurements and by density functional theory calculations. For the ODT junction (Fig. 3(c)), peaks were reproducibly observed at 92, 119, 143, 161, 181, and 355 mV, which correspond to $\nu(\text{C-S})$ stretching, $\delta_r(\text{CH}_2)$ rocking, $\nu(\text{C-C})$ stretching, $\gamma_w(\text{CH}_2)$ wagging, $\delta_s(\text{CH}_2)$ scissoring, and $\nu(\text{C-H})$ stretching modes, respectively. The absence of a prominent peak corresponding to the $\nu(\text{S-H})$ stretching mode at 319 mV (2575 cm^{-1}) suggests that the thiol ($-\text{SH}$) anchoring group reacts with the Au electrode pairs broken during the electromigration. In the IETS spectrum of the BDT junction (Fig. 3(f)), three prominent peaks reproducibly appeared at 96, 142, and 201 mV, corresponding to $\gamma(\text{C-H})$ aryl out-of-plane bending, $\nu(18a)$ stretching, and $\nu(8a)$ stretching modes, respectively. These modes originate from vibrations of the phenyl ring. A theoretical study predicted that the $\nu(18a)$ and the $\nu(8a)$ ring modes should have strong vibronic coupling in phenylene molecules [18] and is consistent with these results. The dominance of aromatic ring modes in IETS spectra has also been experimentally observed for various conjugated molecules [19,21]. The fully-assigned IETS spectrum provides unambiguous experimental evidence for the existence of the desired molecules in the region of the junction and correlates with the other characteristics of the junction transport, thus leaving the IETS-identified molecule as the only element in the junction through which tunneling is occurring.

An important way to verify that the obtained spectra are indeed valid IETS data is to examine the vibrational peaks width broadening as a function of the temperature and the applied modulation voltage. The width of a spectral peak includes a natural intrinsic linewidth, W_I , and two broadening effects: thermal broadening ($5.4 k_B T/e$, where k_B is Boltzmann's constant and T denotes temperature) due to the breadth of the Fermi level and modulation broadening ($1.7 V_m$, where V_m is the AC modulation voltage) due to the dynamic detection technique used to obtain the second-harmonic signals [15]. The full width at half maximum (FWHM) of the d^2I/dV^2 vibrational peak in IETS is given by [23]

$$W = [(1.7 V_m)^2 + (5.4 k_B T/e)^2 + (W_I)^2]^{1/2}. \quad (1)$$

Figure 4 illustrates a study of the linewidth broadening of a vibrational peak in IETS measurements. Figure 4(a) shows the modulation broadening of a representative IETS feature (from Ref. 24, the $\nu(\text{C-H})$ stretching mode of ODT molecules in the electromigrated break junction) at a constant temperature of 4.2 K. The data points show the FWHM of the experimental peak. Considering the known thermal broadening and modulation broadening, we can determine the intrinsic linewidth, W_I , from a fit to the modulation broadening data (Fig. 4(a), solid line), giving $W_I = 4.94 \pm 0.89 \text{ meV}$ (following Eq. (1)). Fig-

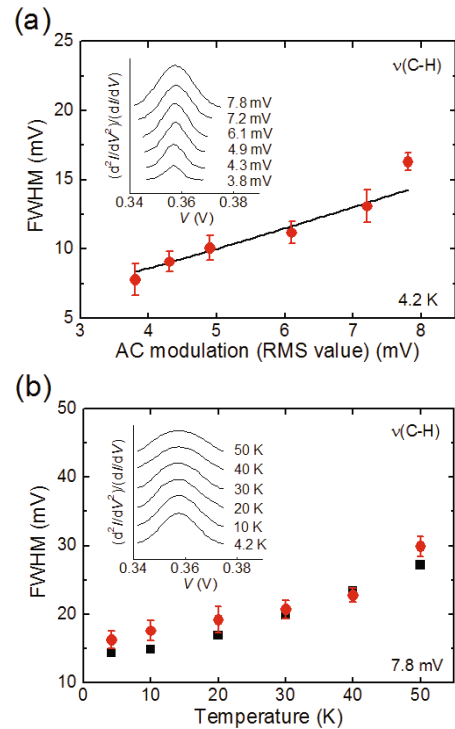


Fig. 4. (Color online) FWHM of the peak corresponding to the $\nu(\text{C-H})$ stretching mode ($\sim 357 \text{ mV}$) as a function of the (a) AC modulation voltage and (b) temperature. The circles indicate experimental data, and the (a) solid line and (b) squares show theoretical values. The error bars are determined by the Gaussian fitting. Insets, successive IETS scans for the $\nu(\text{C-H})$ mode under (a) increasing AC modulation voltage and (b) increasing temperature, as indicated. r.m.s., root mean squared. Reproduced with permission from [24]. Copyright 2009 Nature Publishing Group.

ure 4(b) shows the thermal broadening of the same $\nu(\text{C-H})$ peak at a fixed modulation, demonstrating excellent agreement between the experimental FWHM values (circles) and the theoretical values (squares). This linewidth broadening study clearly indicates that the IETS spectra originate from intrinsic molecular vibrational modes, not from noise signals.

The first observation of IETS in a single molecule was obtained in scanning tunneling microscopy (STM) [25, 26]. The possibility of performing IETS studies using STM was discussed soon after its invention [27]. However, due to difficulties in achieving the extreme mechanical stability that is necessary to observe small changes in the tunneling conductance, this technique has only recently been realized [25]. In the STM implementation of IETS, the MIM tunnel junction is replaced by a STM junction consisting of a sharp metallic tip, a vacuum gap, and a surface with the adsorbed molecules. Using STM-IETS, elegant imaging and probing can be performed at the same time, and vibrational spectroscopy studies on a single molecule can be achieved [26]. One of the most fruitful techniques for IETS of molecular

structures arose from the pioneering work of Gregory in 1990 [28], in which a junction between two crossed wires was delicately made by using a deflecting Lorentz force [29]. Kushmerick et al. demonstrated that reproducible molecular junctions could be formed with sufficient stability and robustness for clear IETS signatures [24]. The ease of electrode and molecular exchange has allowed elegant and thorough investigations of structure-function relationships. The technique has also enabled investigations into such areas as selection rules [21] and pathways [22], illustrating the power of IETS in characterizing and understanding nanoscale junctions. Wang et al. also reported an IETS study of an alkanedithiol self-assembled monolayer (SAM) by using a nanometer-scale device (nanopore technique) [13]. Remarkably, the authors were able to verify that the observed spectra were, indeed, valid IETS data by examining the peak width as a function of temperature and AC modulation voltage (refer to the above paragraph). Recently, Hihath *et al.* [30] reported IETS spectra for a single 1,3-propanedithiol molecule by using an STM break junction at cryogenic temperatures. In particular, those authors were able to observe simultaneous changes in the conductance and the vibrational modes of a single molecule as the junction was stretched. That ability allowed them to correlate the changes in the conductance with the changes in the configuration of the single-molecule junction. Moreover, the authors were also able to conduct a statistical analysis of the phonon spectra to identify the most relevant modes. The vibrational modes matched the IR and the Raman spectra well and could be described by using a simple one-dimensional model [30]. Another useful example of IETS for studying molecular junctions was reported by Long *et al.* [19]. That study provided insight into changing transport characteristics resulting from exposure to air. IETS spectra have shown that molecular conduction can be significantly affected by rapid hydration at gold-sulphur contacts. The detrimental effects of hydration on molecular conduction are important for understanding charge transport through gold-thiol molecular junctions exposed to atmospheric conditions.

When combined with mechanically-controllable break-junction (MCBJ) measurements [31–37], IETS has proven to be useful for investigating the correlation between the molecular conformation or orientation and the charge transport properties of molecular junctions. For example, alkanedithiol molecular junctions have been stretched gradually by several Angstrom by using nanofabricated MCBJs (Fig. 5(a)) and Kim *et al.* [38] recently measured IETS spectra of Au-1,6-hexanedithiol (HDT)-Au junctions for different elongation states. As illustrated in Fig. 5(b), a mechanical transition from a *trans* (black line spectra) to a *gauche* (blue line spectra) conformations could be identified [38]. Furthermore, the Au-S stretching mode changed when the single-molecule conductance jumped from high- to low-conductance states (Fig. 5(c)), indicating that the conductance drop originated from a mechanical deformation

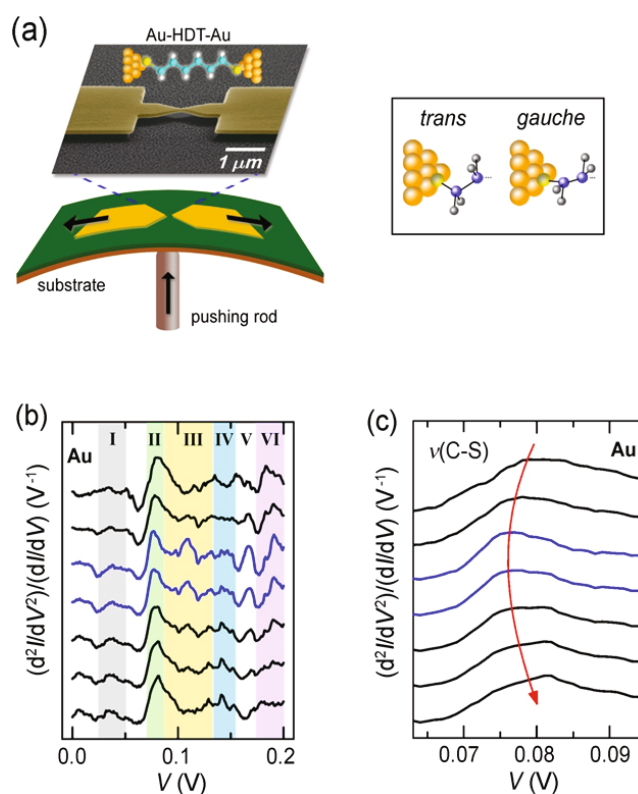


Fig. 5. (Color online) (a) Schematic illustration of the MCBJ system and scanning electron micrograph image of a sample with the scheme of a molecular junction (left). Schematic diagrams of both *trans* and *gauche* conformations (right). (b) IETS spectra displaced vertically in the order of the junction distances in the Au-HDT-Au junction. The IETS are measured between 5 (top) and 14 Å (bottom). (c) Enlarged n(C-S) mode reported in (b). Reproduced with permission from [38]. Copyright 2009 Nature Publishing Group.

of the metal-molecule contact configurations (*e.g.*, formation of a one-dimensional atomic chain or a change in the Au-S bonding distance) [38,39]. That sophisticated study showed that a mechanical strain could be imposed onto the molecular junctions, opening a new route for controlling the charge transport through the vibrational states in individual molecules. IETS combined with the MCBJ technique was also used to investigate the isomerization between the *trans* and the *cis* forms of a photochromic azobenzene-derivatives junction [40].

We recently presented the construction and characterization of molecular transistors [24], where the transport current was controlled by directly modulating the energy of the molecular orbitals of a single molecule (based purely on electrostatic gate control). As illustrated in Fig. 6(a) [41], individual molecules are connected to source and drain electrodes with a bottom-gate control electrode in a field-effect transistor configuration. In such devices, the energies of the molecular orbitals with respect to the Fermi level of the electrodes can be directly tuned by adjusting the gate voltage, V_G . We

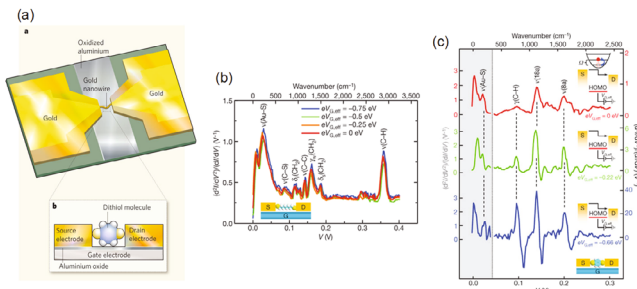


Fig. 6. (Color online) (a) Schematic illustration of a molecular transistor. a, Each device consists of a fractured gold nanowire overlaid on a strip of oxidized aluminum. b, Side-on, close-up view of a device. The broken ends of the nanowire form the source and the drain electrodes of the transistor, and the oxidized aluminum forms the gate electrode. A single molecule (here, an aromatic dithiol) connects the source and the drain electrodes. Reproduced with permission from [41]. Copyright 2010 Nature Publishing Group. (b) IETS spectra for a Au-ODT-Au junction measured at 4.2 K for different values of $eV_{G,eff}$, with vibration modes assigned. (c) IETS spectra for a Au-BDT-Au junction measured at 4.2 K for different values of $eV_{G,eff}$, with vibration modes assigned. The left-hand y axis corresponds to the grey shaded region of the spectra, and the various right-hand y axes (with different scales) correspond to the related (color-coded) spectra in the non-shaded region. The vertical dotted line corresponds to $V = 45$ mV (363 cm^{-1}). Significant modifications in the spectral intensity and line shape for the benzene ring modes, $\gamma(\text{C-H})$, $\nu(18a)$ and $\nu(8a)$, were observed for different values of $eV_{G,eff}$, as indicated. The insets show energy diagrams illustrating inelastic tunneling as the position of the HOMO resonance shifts as a result of gating. Reproduced with permission from [24]. Copyright 2009 Nature Publishing Group.

made such devices by using the electromigration technique of fracturing a continuous gold wire (coated with the desired molecules in vacuum at 4.2 K) that had been over an oxidized aluminum gate electrode [41–43]. This arrangement produced source and drain electrodes with nanometer-scale gaps that were often bridged by a single molecule or by very few molecules. IETS was used to measure the interactions between the tunneling charge carriers and the vibrational modes of the molecules in the devices. This technique provided definitive proof that the measured currents actually passed through the molecules in the molecular transistors.

We further examined the dependence of the IETS spectra on molecular orbital gating [41]. The IETS spectra of transistors that incorporated alkanedithiol (ODT) were essentially unaffected by the gate voltage (Fig. 6(b)). That finding indicated that charge transport through the device was non-resonant; that is, a large energy difference existed between the dithiols HOMO (highest occupied molecular orbital) and the electrode’s Fermi level. Conversely, we observed that the applied gate voltage strongly modulates the IETS spectra of transistors that incorporate an aromatic dithiol (BDT) (Fig. 6(c)) [41]. Specifically, when a negative gate voltage was applied

(which brought the energy of the molecular junction’s HOMO closer to that of the electrode’s Fermi level), the signal intensities of the spectra increased greatly, and the shapes of the vibrational peaks changed. The change in the peak shape is a clear indication of increased coupling between the tunneling charge carriers and the molecular vibrations owing to a near resonance between the HOMO and the Fermi level [44,45].

IV. CONCLUSION

Over the last few years, IETS has evolved into an essential tool in the field of molecular electronics. Although IETS requires cryogenic temperatures, it is the only method that provides both structural and electronic information about a single-molecule electronic device for a particular conformation and contact geometry of the molecular junction at low temperature. With sophisticated comparisons between experiments and theoretical computations, IETS can be more useful for characterizing numerous aspects of molecular junctions, such as the identification of the molecule, the nature of the interfaces, the orientation of the molecule, and even electronic pathways in those junctions.

ACKNOWLEDGMENTS

This work was supported by a grant from Kyung Hee University (KHU- 20130570), the US Army Research Office (W911NF-08-1-0365), the Canadian Institute for Advanced Research, and the National Science Foundation. An author (T.L.) appreciates the financial support from the National Creative Research Laboratory program (Grant No. 2012026372) of Korea.

REFERENCES

- [1] H. Song, M. A. Reed and T. Lee, *Adv. Mater.* **23**, 1583 (2010).
- [2] N. J. Tao, *Nat. Nanotechnol.* **1**, 173 (2006).
- [3] H. B. Akkerman and B. de Boer, *J. Phys.: Condens. Matter* **20**, 013001 (2008).
- [4] S. J. van der Molen and P. Liljeroth, *J. Phys.: Condens. Matter* **22**, 133001 (2010).
- [5] J. C. Cuevas and E. Scheer, *Molecular Electronics: An Introduction to Theory and Experiment* (World Scientific, Singapore, 2009).
- [6] M. A. Reed and T. Lee, *Molecular Nanoelectronics* (American Scientific, Stevenson Ranch, 2003).
- [7] J. R. Heath, *Annu. Rev. Mater. Res.* **39**, 1 (2009).
- [8] R. L. McCreery, A. J. Bergren, *Adv. Mater.* **21**, 4303 (2009).
- [9] J. Lambe and R. C. Jaklevic, *Phys. Rev.* **165**, 821 (1968).

- [10] R. C. Jaklevic and J. Lambe, *Phys. Rev. Lett.* **17**, 1139 (1966).
- [11] M. A. Reed, *Mater. Today* **11**, 46 (2008).
- [12] M. Galperin, M. A. Ratner, A. Nitzan and A. Troisi, *Science* **319**, 1056 (2008).
- [13] W. Wang, T. Lee, I. Kretzschmar and M. A. Reed, *Nano Lett.* **4**, 643 (2004).
- [14] J. G. Kushmerick, J. Lazorcik, C. H. Patterson, R. Shashidhar, D. S. Seferos and G. C. Bazan, *Nano Lett.* **4**, 639 (2004).
- [15] P. K. Hansma, *Phys. Lett. C Phys. Rep.* **30**, 145 (1977).
- [16] T. Horiuchi, F. Ebisawa and H. Tabei, *Rev. Sci. Instrum.* **60**, 993 (1989).
- [17] H. Song, Y. Kim, J. Ku, Y. H. Jang, H. Jeong and T. Lee, *Appl. Phys. Lett.* **94**, 103110 (2009).
- [18] A. Troisi, M. A. Ratner and A. Nitzan, *J. Chem. Phys.* **118**, 6072 (2003).
- [19] D. P. Long, J. L. Lazorcik, B. A. Mantoosh, M. H. Moore, M. A. Ratner, A. Troisi, Y. Yao, J. W. Ciszek, J. M. Tour and R. Shashidhar, *Nat. Mater.* **5**, 901 (2006).
- [20] H. Song, Y. Kim, H. Jeong, M. A. Reed and T. Lee, *J. Phys. Chem. C* **114**, 20431 (2010).
- [21] J. M. Beebe, H. J. Moore, T. R. Lee and J. G. Kushmerick, *Nano Lett.* **7**, 1364 (2007).
- [22] A. Troisi, J. M. Beebe, L. B. Picraux, R. D. van Zee, D. R. Stewart, M. A. Ratner and J. G. Kushmerick, *Proc. Natl. Acad. Sci. USA* **104**, 14255 (2007).
- [23] L. J. Lauhon and W. Ho, *Rev. Sci. Instrum.* **72**, 216 (2001).
- [24] H. Song, Y. Kim, Y. H. Jang, H. Jeong, M. A. Reed and T. Lee, *Nature* **462**, 1039 (2009).
- [25] B. C. Stipe, M. A. Rezaei and W. Ho, *Science* **280**, 1732 (1998).
- [26] W. Ho, *J. Chem. Phys.* **117**, 11033 (2000).
- [27] G. Binnig, N. Garcia and H. Rohrer, *Phys. Rev. B* **32**, 1336 (1985).
- [28] S. Gregory, *Phys. Rev. Lett.* **64**, 689 (1990).
- [29] J. G. Kushmerick, D. B. Holt, J. C. Yang, J. Naciri, M. H. Moore and R. Shashidhar, *Phys. Rev. Lett.* **89**, 086802 (2002).
- [30] J. Hihath, C. R. Arroyo, G. Rubio-Bollinger, N. J. Tao and N. Agrait, *Nano Lett.* **8**, 1673 (2008).
- [31] J. Moreland and J. W. Ekin, *J. Appl. Phys.* **58**, 3888 (1985).
- [32] C. J. Muller, J. M. van Ruitenbeek and L. J. de Jongh, *Physica C* **191**, 485 (1992).
- [33] R. Huber, M. T. Gonzalez, S. Wu, M. Langer, S. Grunder, V. Horhoiu, M. Mayor, M. R. Bryce, C. S. Wang, R. Jitchati, C. Schonenberger and M. J. Calame, *J. Am. Chem. Soc.* **130**, 1080 (2008).
- [34] S. Wu, M. T. Gonzalez, R. Huber, S. Grunder, M. Mayor, C. Schönenberger and M. Calame *Nat. Nanotech.* **3**, 569 (2008).
- [35] M. T. Gonzalez, S. Wu, R. Huber, S. J. van der Molen, C. Schönenberger and M. Calame, *Nano Lett.* **6**, 2238 (2006).
- [36] E. Lörtscher, H. Weber and H. Riel, *Phys. Rev. Lett.* **98**, 176807 (2007).
- [37] M. A. Reed, C. Zhou, C. J. Muller, T. P. Burgin and J. M. Tour, *Science* **278**, 252 (1997).
- [38] Y. Kim, H. Song, F. Strigl, H.-F. Pernau, T. Lee and E. Scheer, *Phys. Rev. Lett.* **106**, 196804 (2011).
- [39] Y. Kim, T. J. Hellmuth, M. Burkle, F. Pauly and E. Scheer, *ACS Nano* **5**, 4104 (2011).
- [40] Y. Kim, A. Garcia-Lekue, D. Sysoiev, T. Frederiksen, U. Groth and E. Scheer, *Phys. Rev. Lett.* **109**, 226801 (2012).
- [41] J. Kushmerick, *Nature* **462**, 994 (2009).
- [42] E. A. Osorio, K. O'Neill, M. Wegewijs, N. Stuhr-Hansen, J. Paaske, T. Bjørnholm and H. S. J. van der Zant, *Nano Lett.* **7**, 3336 (2007).
- [43] J. Park, A. N. Pasupathy, J. I. Goldsmith, C. Chang, Y. Yaish, J. R. Petta, M. Rinkoski, J. P. Sethna, H. D. Abruna, P. L. McEuen and D. C. Ralph, *Nature* **417**, 722 (2002).
- [44] M. Galperin, M. A. Ratner and A. J. Nitzan, *J. Chem. Phys.* **121**, 11965 (2004).
- [45] B. N. J. Persson and A. Baratoff, *Phys. Rev. Lett.* **59**, 339 (1987).